Chemical Engineering Journal 224 (2013) 39–45

Contents lists available at SciVerse ScienceDirect

Chemical Engineering Journal

journal homepage: www.elsevier.com/locate/cej

Modeling of a bench-scale photocatalytic reactor for water disinfection from laboratory-scale kinetic data

Javier Marugán [a,*], Rafael van Grieken [a,1], Cristina Pablos [a,1], M. Lucila Satuf [b,2], Alberto E. Cassano [b,2], Orlando M. Alfano [b,2]

[a] Department of Chemical and Environmental Technology, ESCET, Universidad Rey Juan Carlos, C/Tulipán s/n, 28933 Móstoles, Madrid, Spain
[b] Instituto de Desarrollo Tecnológico para la Industria Química (INTEC), Universidad Nacional del Litoral-CONICET, CCT Santa Fe, Paraje El Pozo, Colectora de la Ruta Nacional No. 168, 3000 Santa Fe, Argentina

HIGHLIGHTS

- Novel predictive tool for the simulation of photoreactors for water disinfection.
- Reactor simulation based on geometry, irradiation source operation conditions.
- The only experimental data are the kinetic parameters calculated at lab scale.
- Successful validation of the experimental predictions in a bench-scale reactor.
- Agreement between experimental and predicted optimal catalyst concentration.

ARTICLE INFO

Article history:
Available online 28 November 2012

Keywords:
Photocatalysis
Disinfection
Photoreactor
Mass transport
Kinetics
E. coli

ABSTRACT

A model of a bench-scale, annular, continuous flow reactor for the photocatalytic disinfection of water, operated under conditions of no perfect mixing is presented. The performance of the photoreactor has been simulated following a predictive procedure, with no adjustable parameters, based on the intrinsic kinetics and the information about the geometry, irradiation source and operation conditions (catalysts concentration and its properties as well as the initial concentration of bacteria). The only experimental information required to be determined at laboratory scale are the kinetic parameters of a mechanistic model that takes into account the explicit dependence of the reaction rate with respect to the local volumetric rate of photon absorption (LVRPA) and the optical properties of the catalyst. The proposed model predicts an optimal catalyst concentration in the range $0.1–0.2 \times 10^{-3}$ g cm^{-3}, with a significant decrease in the disinfection efficiency for higher catalyst loadings. Important resistances to the mass transport are detected at high TiO_2 concentrations, as a result of the low diffusion coefficient of the employed microorganism (*Escherichia coli*). Operating under the optimal catalyst concentration, model predictions show satisfactory agreement with experimental results extracted from the custom-built bench scale reactor.

1. Introduction

The procedures commonly used for designing large chemical reactors are usually based on the preliminary determination of the reaction kinetics at laboratory scale, in which ideal well-mixed and isothermal conditions for the reaction can be readily obtained. Under these circumstances, experimental values for the kinetic constant of a given kinetic model of the process at different temperatures can be calculated, including the determination of the activation energy through the Arrhenius equation. Once the kinetics of the process is determined, it can be applied to the simulation of larger and even non-isothermal reactors, being only required the simultaneous determination of the temperature and concentration profiles for the calculation of the reaction rate at each local position of the reactor.

In contrast to thermally-activated processes, photo-activated reactions have introduced significant difficulties to the reactor design procedure. Some of them are derived from the directional nature of radiation in comparison with temperature, making the thermal energy balances used in temperature or catalytic promoted processes much more difficult, because it is necessary to include the radiation energy conservation equation even in

* Corresponding author. Tel.: +34 91 664 7466; fax: +34 91 488 7068.
E-mail addresses: javier.marugan@urjc.es (J. Marugán), alfano@intec.unl.edu.ar (O.M. Alfano).
[1] Tel.: +34 91 664 7466; fax: +34 91 488 7068.
[2] Tel.: +54 342 451 1372/73; fax: +54 342 451 1087.

1385-8947/$ - see front matter © 2012 Elsevier B.V. All rights reserved.
http://dx.doi.org/10.1016/j.cej.2012.11.082

Nomenclature

B	bacteria
C	bacteria concentration, CFU cm^{-3}
C_{cat}	catalyst mass concentration, g cm^{-3}
$D^0_{E.coli-Water}$	diffusivity of *E. coli* bacteria in water, $cm^2\ s^{-1}$
e^a	local volumetric rate of photon absorption, Einstein $cm^{-3}\ s^{-1}$
L	nominal reactor length, cm
r	radial cylindrical coordinate, cm
R	volumetric reaction rate for bacteria, CFU $cm^{-3}\ s^{-1}$
S_g	TiO_2 specific surface area of the catalyst, $cm^2\ g^{-1}$
t	time, s
v_z	axial velocity, cm s^{-1}
V	volume, cm^3
$\underline{x}$	position vector in a 3D space, cm
z	axial cylindrical coordinate, cm

Greek letters

α	kinetic parameter, units depend on the specific kinetic model
α_2	kinetic parameter, cm^2 s Einstein^{-1}
α_3	kinetic parameter, dimensionless
α_4	kinetic parameter, dimensionless
τ	residence time, s

Subscripts

0	indicates initial condition
cat	relative to the catalyst
d	relative to damaged bacteria
ext	relative to the external wall of the reactor
i	relative to inactivated bacteria
int	relative to the internal wall of the reactor
Reactor	relative to the reactor
Total	relative to the total recirculating system
Tank	relative to the reservoir tank
u	relative to undamaged bacteria
V_{React}	relative to the reactor volume

Superscript

inlet	relative to the inlet stream

Special symbols

_	indicates a vector magnitude
[ ]	concentration of bacteria species in the bulk, CFU cm^{-3}
⟨ ⟩	indicates average value

isothermal systems. The main difficulty falls in the practical impossibility of achieving isoactinic conditions (that would be equivalent to the isothermal one in thermal reactors) even in very small laboratory photoreactors. Consequently, the determination of kinetic parameters for photo-activated reactions necessarily requires the simultaneous description of the unavoidable radiation profiles existing inside the photoreactor, because the reaction rate will normally be much higher in the regions of high irradiation near the radiation entrance wall as compared with others that are further away and consequently increasingly darker.

Most of the reports on the photocatalytic degradation of chemical pollutants or the photocatalytic inactivation of microorganisms found in the literature used very simple equations such as pseudo-first order or Langmuir–Hinshelwood kinetic models that only take into account the concentration of the reactants. The effect of the catalyst concentration and radiation absorption is considered only implicitly in the macroscopic volume-averaged kinetic constant calculated from the fitting of the experimental data. Consequently the derived kinetic expressions are only valid for the experimental setup in which have been developed, they cannot be extrapolated to other reactor configurations and, therefore, they are absolutely useless for photoreactor design purposes. The kinetic models required for scaling-up or designing photochemical reactors must be independent of the shape and configuration of the reactor and based on the detailed reaction mechanism of the process, with parameters based on phenomenological or mechanistic basis, including the radiation activated steps and therefore the spatial distribution of the photon absorption rate [1–4].

Previous papers have reported different approaches for the development of scaling-up strategies for photocatalytic reactors [2,5–9]. However, none of them have been experimentally verified for disinfection applications, being the photocatalytic inactivation of microorganisms a process much more difficult to interpret than conventional oxidation of chemical pollutants. In the case of microbiological reactors, even before attempting to perform a scale-up for designing an apparatus under production conditions, there is an issue that should be carefully analyzed: the significantly different size of typical chemical molecules and microorganisms. In our previous kinetic model [10], we were forced to introduce an assumption never used before and to consider that the catalyst was adsorbed on the surface of the microbial cell. This leads us to wonder to what extent this assumption could impose restrictions in mass transport, and give rise to a major constraint in the design of reactors that are not operated in situations of perfect mix.

In a previous work [11], we reported that the photocatalytic inactivation of bacteria could be represented by the following simplified reaction scheme:

$$B_u \rightarrow B_d \rightarrow B_i \rightarrow \text{Products} \quad (1)$$

where B_u represents the undamaged bacteria, B_d the damaged but still viable bacteria, and B_i the inactivated bacteria.

The small reactor volume and the relatively slow kinetics of the disinfection process allow the following assumptions: (i) the system is perfectly mixed; (ii) there are no mass transport limitations; and (iii) the conversion per pass in the reactor is differential. Under these special conditions, the flow regime has almost no effect on the kinetics and, consequently, in the interpretation of the experimental data. Thus, the mass balance of viable bacteria in the reservoir tank can be expressed as follows:

$$\left.\frac{d[B_u](t)}{dt}\right|_{Tank} = \frac{V_{Reactor}}{V_{Total}}\langle R_u(\underline{x},t)\rangle_{V_{Reactor}} \quad t=0 \quad [B_u]=[B]_0 \quad (2)$$

$$\left.\frac{d[B_d](t)}{dt}\right|_{Tank} = \frac{V_{Reactor}}{V_{Total}}\langle R_d(\underline{x},t)\rangle_{V_{Reactor}} \quad t=0 \quad [B_d]=0 \quad (3)$$

where $V_{Reactor}$ is the irradiated reactor volume; V_{Total} is the total suspension volume; t denotes reaction time; and $\langle R_i(\underline{x},t)\rangle_{V_{Reactor}}$ is the volumetric rate of undamaged ($i=u$) and damaged ($i=d$) bacteria disappearance averaged over the whole reactor volume.

The reaction rate of bacterial inactivation must be estimated through the use of a kinetic model based on the intrinsic reaction mechanism that takes into account explicitly radiation absorption steps. A suitable mechanism was proposed in a previous work [10], leading to successful development of a kinetic model that was able to reproduce the experimental data of *Escherichia coli* photocatalytic inactivation under a wide range of operation conditions of

catalyst concentration, irradiation power and initial concentration of bacteria. This model can be represented by the two following kinetic expressions:

$$R_u\left(\frac{\text{CFU}}{\text{s cm}^3}\right) = -\alpha C_{cat}\frac{[B_u]^2}{[B_u]+\alpha_4[B_d]+\alpha_3([B]_0-[B_u]-[B_d])}\left[-1+\sqrt{1+\frac{\alpha_2 e^a}{S_g C_{cat}}}\right] \quad (4)$$

$$R_d\left(\frac{\text{CFU}}{\text{s cm}^3}\right) = \alpha C_{cat}\frac{[B_u]^2-\alpha_4[B_d]^2}{[B_u]+\alpha_4[B_d]+\alpha_3([B]_0-[B_u]-[B_d])}\left[-1+\sqrt{1+\frac{\alpha_2 e^a}{S_g C_{cat}}}\right] \quad (5)$$

where R_u and R_d are the reaction rate for undamaged and damaged bacteria, respectively, $[B_u]$ and $[B_d]$ are the concentration of undamaged and damaged bacteria, $[B]_0$ is the initial concentration of bacteria, e^a is the local volumetric rate of photon absorption (LVRPA), S_g is the catalyst specific surface area, C_{cat} is the catalyst mass concentration, and α, α_2, α_3, α_4 are kinetic parameters. The details of the derivation of the kinetic model and the assumptions considered to obtain the kinetic expressions can be found in the literature [10]. It has to be highlighted that this model provides a general rate expression with an explicit dependence of the bacterial inactivation on the photon absorption, taking into account the spatial variations of the LVRPA produced by the unavoidable radiation profiles existing in the photoreactor.

The values of the intrinsic kinetic parameters of Eqs. (4) and (5) can be estimated using a nonlinear regression algorithm to fit the experimental data obtained in the laboratory scale reactor to the predictions of the model calculated by resolution of the mass balance Eqs. (2) and (3), considering that the experimental C/C_0 results correspond to the computed $([B_u](t)+[B_d](t))/[B]_0$ values. The kinetic parameters that best reproduce the experimental data obtained in a range of catalyst concentration from 0.02×10^{-3} to 0.2×10^{-3} g cm^{-3}, irradiation power from 0.778×10^{-7} to 2.72×10^{-6} Einstein s^{-1}, and initial concentration of bacteria from 10^3 to 10^6 CFU cm^{-3} are [10]:

$$\alpha = (7.82\pm0.35)\times10^{1}\ \text{cm}^3\ \text{g}^{-1}\ \text{s}^{-1} \quad (6)$$

$$\alpha_2 = (3.66\pm0.43)\times10^{11}\ \text{cm}^2\ \text{s Einstein}^{-1} \quad (7)$$

$$\alpha_3 = (2.44\pm0.51)\times10^{-6} \quad (8)$$

$$\alpha_4 = (1.28\pm0.53)\times10^{-1} \quad (9)$$

The objective of this work is to carry out the study of the disinfection reaction of *E. coli* with titanium dioxide and UV radiation in an annular, continuous flow reactor that is not operated under conditions of perfect mixing. This procedure intends to detect from which operating conditions important resistances to the mass transport will be highlighted. This information will be used to check if they correspond to situations usually expected during the scale-up operation.

2. Experimental

2.1. Laboratory and bench scale photoreactors

The experimental setup for the photocatalytic reactions used for the estimation of the intrinsic kinetic parameters consists of an annular photoreactor made of borosilicate glass (main dimensions and characteristics are summarized in Table 1). The system operates in a closed recirculating circuit driven by a centrifugal pump with a suspension flow rate of 2.5 L min^{-1}. Although the reactor is theoretically operating under laminar flow regime, the short length of the reactor and the turbulence generated at the reactor entrance (the inlet suspension impact directly against the reactor wall) assure good mixing conditions. The total working volume of the system including the well-stirred reservoir tank where samples are withdrawn is 1 L. Good aeration conditions were maintained in the reservoir tank to provide a concentration of dissolved oxygen above 90% of the saturation limit. As the conversion per pass is almost negligible, the consumption of oxygen inside the reactor can be neglected and considered constant and not limiting the reaction rate. A Philips TL 6W/08 black light blue lamp with a maximum emission at 370–375 nm was placed in the axis of the annulus, controlling the irradiation power entering the reactor through the use of neutral filters. More details about the reactor, filters, emission spectrum of the lamp and quantitative values of the radiation fluxes determined by ferrioxalate actinometry can be found elsewhere [10].

Table 1
Dimensions and characteristics of the laboratory and bench scale reactors.

Description	Laboratory scale reactor	Bench scale reactor
Main dimensions	Length = 15.0 cm Inner diameter = 3.0 cm Outer diameter = 5.0 cm	Length = 100.0 cm Inner diameter = 3.0 cm Outer diameter = 5.0 cm
Reactor volume	188.5 cm^3	1250 cm^3
Total system volume	1000 cm^3	4000 cm^3
Recirculation flow rate	41.7 cm^3 s^{-1}	65 cm^3 s^{-1}
Reynolds number	665	1035
Lamp type	Black light fluorescent Philips TL 6W/08	Black light fluorescent Osram L 36 W/73 FLH1
Lamp position	Axial	Axial
Lamp dimensions	Length = 21.0 cm[a] Diameter = 1.6 cm	Length = 120.0 cm[b] Diameter = 2.6 cm
Electrical input power	6 W	36 W
UV emission range	350–400 nm	350–400 nm
Total radiation flow	0.778–2.72×10^{-6} Einstein s^{-1}	1.8×10^{-5} Einstein s^{-1}
Inlet radiation surface	141.4 cm^2	942.5 cm^2
Radiation flux	0.550–1.92×10^{-8} Einstein cm^{-2} s^{-1}	1.91×10^{-8} Einstein cm^{-2} s^{-1}

[a] Lamp positioned at z = 3 cm to minimize end effects.
[b] Lamp positioned at z = 10 cm to minimize end effects.

The bench-scale photoreactor setup is also a borosilicate annular photoreactor operating in a closed recirculating circuit with an Osram L 36 W black light lamp placed in the axis of the reactor. From its main dimensions and characteristics (also summarized in Table 1) it can be seen that, with reference to the laboratory scale reactor, the irradiated volume was increased from 188.5 to 1250 cm^3 and the total irradiation power from 2.72×10^{-6} to 1.8×10^{-5} Einstein s^{-1}. A scheme of the experimental reactor setup is shown in Fig. 1.

2.2. Reaction procedure

E. coli K-12 strains provided by the Colección Española de Cultivos Tipo (CECT 4624, corresponding to ATCC 23631) was used as model microorganism. *E. coli* is frequently used as fecal contamination indicator to evaluate the microbiological quality of water, and its presence in water is typically regulated by legislation. K12 is an *E. coli* strain well-adapted to the laboratory environment, and, unlike wild type strains, has lost its ability to thrive in the intestine, making safer the experimental work. Fresh liquid cultures with a stationary concentration around 10^9 colony forming units (CFU) mL^{-1} were prepared by inoculation in a Luria–Bertani nutrient medium

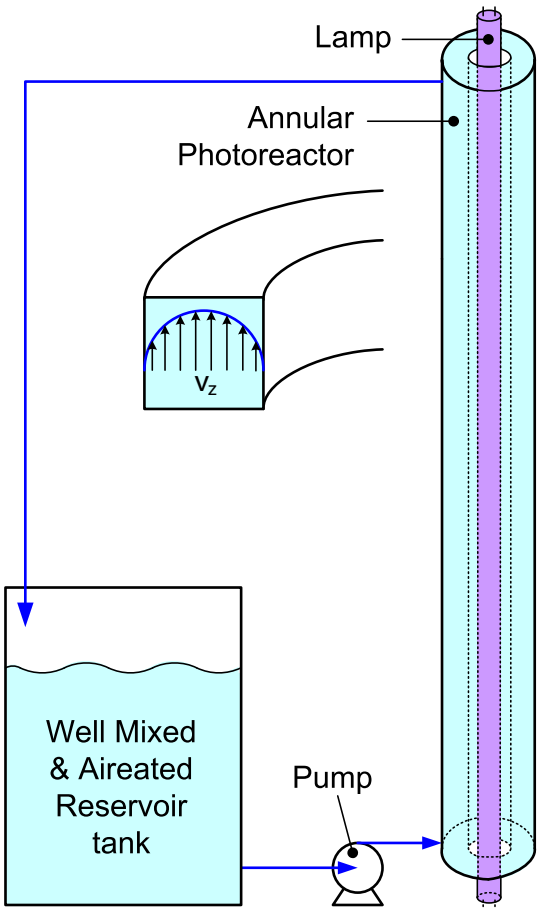

Fig. 1. Scheme of the bench scale reactor setup.

(Miller's LB Broth, Scharlab) and aerobic incubation at 37 °C for 24 h under constant stirring on a rotary shaker. Reacting suspensions were prepared by centrifuging 5 mL of the liquid culture at 3000 rpm for 15 min, rinsing twice the bacteria with 5 mL of sterile ultra-pure water (Milli-Q®, 18.2 MΩ cm) and finally diluting the required amount of aqueous *E. coli* suspension to get an initial concentration of viable bacteria in the range of 10^3–10^6 CFU mL^{-1}.

Disinfection experiments have been carried out using suspensions of Evonik Aeroxide® TiO_2 P 25 (formerly known as Degussa P25 TiO_2). This photocatalyst has been widely studied in the literature and it is usually considered as a standard in photocatalytic reports. Its physicochemical and optical properties, required for the radiation model of the reactor operation, have been previously reported [12,13]. The absorption spectra of the suspensions of this material have a reasonable degree of overlapping with the emission spectrum of the lamps used in the photoreactors [10], allowing the activation of the photocatalytic process.

The experimental procedure used with both reactors was similar. The bacterial suspension and the catalyst were charged in the reservoir tank and the recirculation pump was switched on 15 min for the equilibration of the system. In the meantime, the lamp was switched on outside the reactor to stabilize its emission power and spectrum before the reaction starts. The evolution of the reaction was followed quantifying the concentration of viable bacteria by a standard serial dilution method using LB nutrient agar plates (Miller's LB Agar, Scharlab), using eight independent measurements of each sample to obtain statistically significant data. Additionally, key experiments were repeated three times to test the reproducibility of the disinfection results. More details of the procedure can be found elsewhere [14].

3. Results and discussion

The simulation of the performance of a photocatalytic reactor, independently of its size, starts with the determination of the radiation field, in order to calculate the LVRPA values (e^a) in each discrete position of the system required for the calculation of the reaction rate with the kinetic model expressions (4) and (5). Radiation calculations can be done through the resolution of the Radiative Transfer Equation (RTE) that describes the transport of photons inside the reactor. A detailed description of the numerical procedure for the resolution of the RTE in cylindrical photoreactors using a 2-dimensional 2-directional radiation model can be found elsewhere [4]. The inlet radiation, boundary condition for the resolution of the RTE, has been estimated from the total incident radiation determined by actinometry following: (i) wavelength discretization based on the lamp emission spectrum; and (ii) directional discretization using a superficial diffuse emission model of the tubular lamp and taking into account the geometry of the system [15]. Assuming that the optical properties of the suspension do not vary throughout the reaction, the LVRPA distribution evaluated on the photoreactor can be considered constant.

The evolution of the concentration of viable bacteria in the reservoir tank can be calculated from the resolution of the mass balance equation, in similar way that it has been explained for the laboratory reactor. However, in this case, the larger size of the reactor and the flow regime do not allow the consideration of the whole recirculating system as perfectly mixed. Assuming well mixing conditions in the reservoir tank, the mass balance in non-steady state that describes the evolution with time of the concentration of undamaged and damaged bacteria in the tank takes the following expression:

$$\left.\frac{d[B_u](t)}{dt}\right|_{Tank} = \frac{1}{\tau_{Tank}}([B_u]^{inlet}(t) - [B_u](t)) \quad t = 0 \quad [B_u] = [B]_0 \qquad (10)$$

$$\left.\frac{d[B_d](t)}{dt}\right|_{Tank} = \frac{1}{\tau_{Tank}}([B_d]^{inlet}(t) - [B_d](t)) \quad t = 0 \quad [B_d] = 0 \qquad (11)$$

where τ_{Tank} is the residence time in the reservoir tank.

Differential Eqs. (10) and (11) can be been solved using a conventional fourth-order Runge–Kutta numerical method in which the values of the inlet concentration of undamaged and damaged

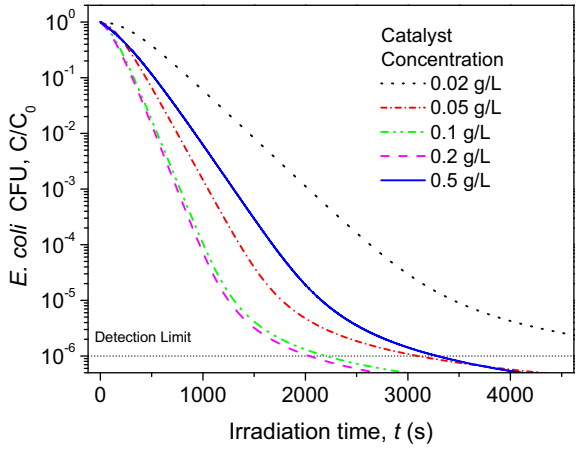

Fig. 2. Model predictions for the photocatalytic inactivation of *E. coli* at the bench scale reactor operating with increasing catalyst concentrations.

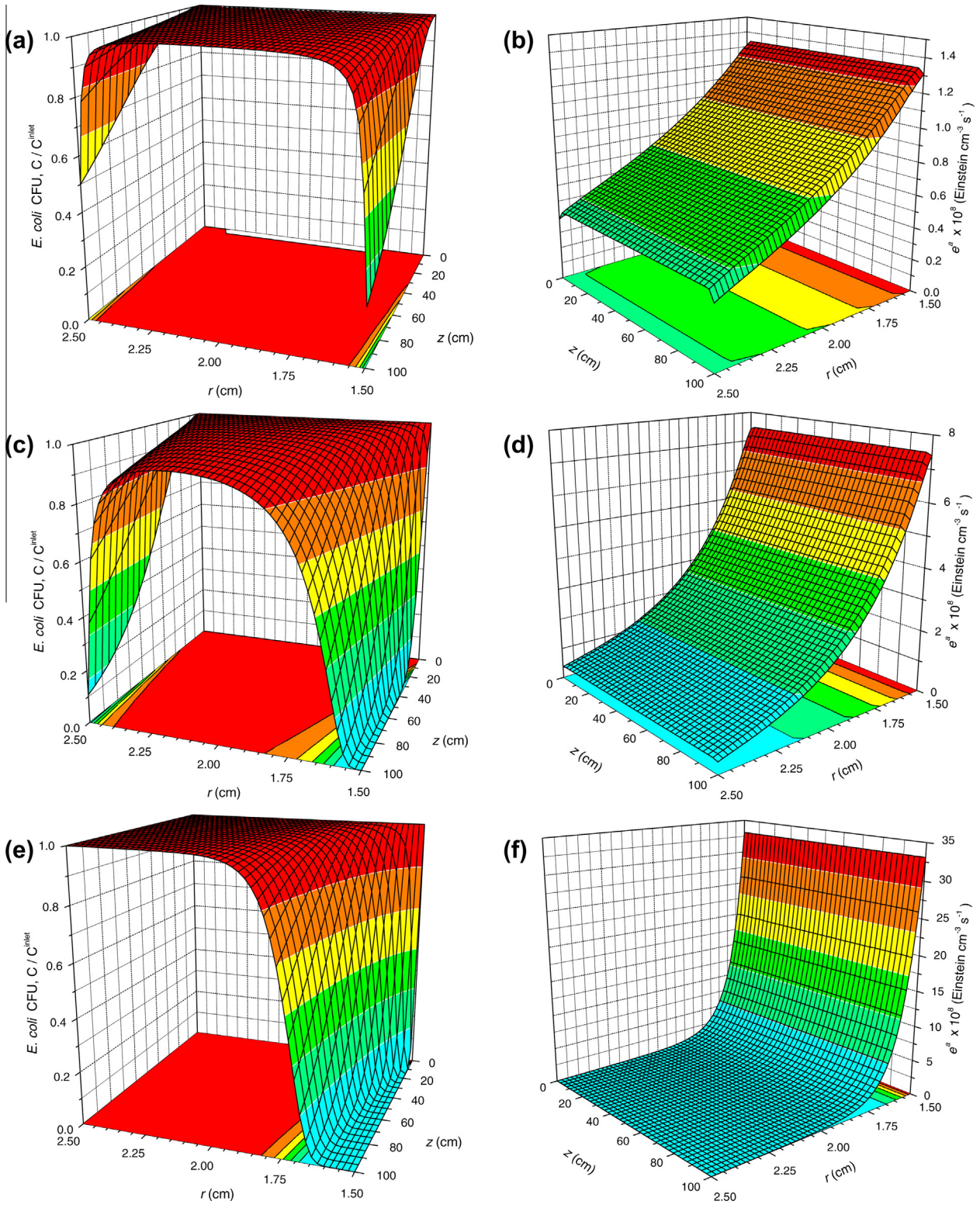

Fig. 3. Concentration profile of viable *E. coli* inside the photoreactor calculated from the resolution of the differential mass balance Eqs. (12) and (13) for undamaged and damaged bacteria at initial concentration of bacteria of 1.0×10^6 CFU cm^{-3} and increasing TiO_2 concentrations of: (a) 0.02×10^{-3} g cm^{-3}; (c) 0.1×10^{-3} g cm^{-3}; (e) 0.5×10^{-3} g cm^{-3}; and LVRPA profiles estimated at these TiO_2 loadings (b) 0.02×10^{-3} g cm^{-3}; (d) 0.1×10^{-3} g cm^{-3}; (f) 0.5×10^{-3} g cm^{-3}.

bacteria are equal to the outlet concentrations of the reactor, calculated through the resolution of its corresponding mass balance at time intervals sufficiently short to be considered at steady state.

The differential form of the mass conservation equation of undamaged and damaged bacteria in the photoreactor has been obtained under the following assumptions: (i) steady state; (ii) negligible thermal effects; (iii) unidirectional axial flow; (iv) azimuthal symmetry; (v) negligible axial diffusion when compared to the convective flux in that direction; (vi) incompressible flow (constant ρ); and (vii) constant diffusion coefficient ($D^0_{E.coli} = 9.2 \times 10^{-7}$ cm^2 s^{-1} [16]). The resulting expressions in cylindrical coordinates are:

$$v_z(r)\frac{\partial[B_u](z,r)}{\partial z} = D^0_{E.coli-Water}\left(\frac{1}{r}\frac{\partial}{\partial r}\left(r\frac{\partial[B_u](z,r)}{\partial r}\right)\right) + R_u(z,r) \quad (12)$$

$$v_z(r)\frac{\partial[B_d](z,r)}{\partial z} = D^0_{E.coli-Water}\left(\frac{1}{r}\frac{\partial}{\partial r}\left(r\frac{\partial[B_d](z,r)}{\partial r}\right)\right) + R_d(z,r) \quad (13)$$

where the reaction rates in each spatial position of the reactor, $R_u(z,r)$ and $R_d(z,r)$, are calculated by the intrinsic kinetic model given by Eqs. (4) and (5). The resolution of Eqs. (12) and (13) can be done through the use of a Crank–Nicholson finite differences scheme with boundary conditions derived from the following assumptions:

(i) The reactor walls are non-permeable:

$$\frac{\partial[B_u](z,r_{int})}{\partial r} = \frac{\partial[B_u](z,r_{ext})}{\partial r} = 0$$
$$\frac{\partial[B_d](z,r_{int})}{\partial r} = \frac{\partial[B_d](z,r_{ext})}{\partial r} = 0 \quad (14)$$

(ii) The inlet concentrations of undamaged and damaged bacteria to the reactor are known and correspond to the outlet concentrations of the tank:

$$[B_u](z=0,r) = [B_u](t) \quad [B_d](z=0,r) = [B_d](t) \quad (15)$$

The resolution of differential mass balances (12)–(15) requires the estimation of the velocity profiles in the annular space, $v_z(r)$, that under the assumptions of: (a) laminar flow regime; (b) Newtonian fluid; and (c) negligible end effects, can be expressed as:

$$v_z(r) = 2\langle v_z\rangle\left(1-(r/r_{ext})^2 + \frac{1-\chi^2}{\ln(1/\chi)} \times \ln(r/r_{ext})\right) \Big/ \left(\frac{1-\chi^4}{1-\chi^2} - \frac{1-\chi^2}{\ln(1/\chi)}\right) \quad (16)$$

where $\langle v_z\rangle$ represents the average velocity, constant under incompressible flow conditions, and $\chi = r_{int}/r_{ext}$.

(iii) The inlet concentrations of undamaged and damaged bacteria to the tank [Eqs. (10) and (11)] are calculated from the corresponding outlet concentrations of the reactor obtained through the resolution of the differential mass balances [Eqs. (12)–(15)].

Fig. 2 shows the predictions for the bacterial concentration evolution in the reservoir tank calculated from the resolution of the model of the bench scale reactor under operation at increasing catalysts concentrations. It can be seen that the model predicts a maximum activity for concentration of TiO_2 in the range 0.1–0.2 $\times 10^{-3}$ g cm^{-3}, with a significant decrease in the disinfection efficiency for higher catalyst loadings.

It is worth mentioning that this optimal catalyst concentration range has not been observed in the laboratory experiments used for the determination of the intrinsic kinetics of the process. This effect of decreasing activity for high catalyst concentrations has been experimentally observed by several research groups in the oxidation of chemical pollutants (e.g. [17]) but for much higher TiO_2 loadings, and it is not typically considered in the standard saturation-shape dependence of the reaction rate on the catalyst concentration [18]. This decrease in the activity for high TiO_2 loadings is indicative of mass transport limitations and should only appear in non-perfectly mixed photoreactor systems. This fact is verified by the axial and radial concentration profiles calculated for the concentration of viable bacteria at different TiO_2 loadings represented in Fig. 3, together with the corresponding LVRPA profiles.

As expected, due to the increase in the residence time, a decrease of the concentration is observed along the z axis of the reactor for a fixed value of r. On the other hand, a strongly non-uniform radial profile is observed, with higher conversions near the reactor

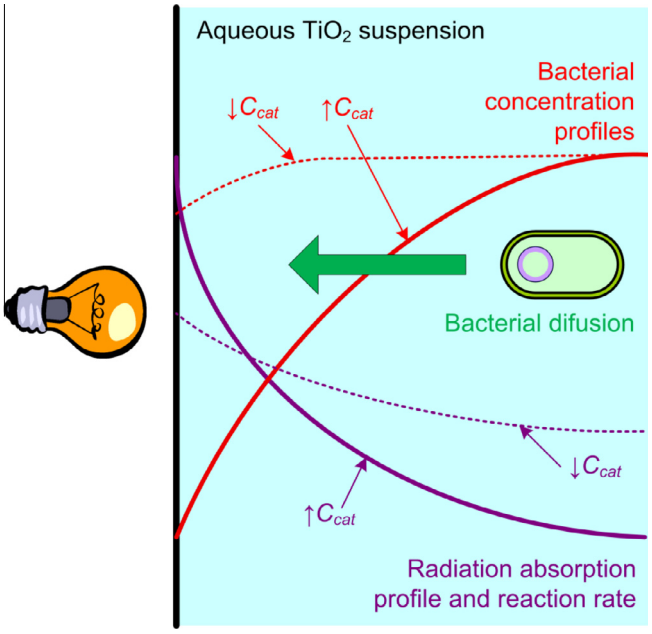

Fig. 4. Schematic representation of radiation and concentration profiles near the irradiated reactor wall (details in the text).

walls (due to the higher residence time derived of the velocity profiles) and with a significantly higher conversion near the irradiated wall at r = 1.5 cm. The increase in the catalyst concentration from 0.02 $\times 10^{-3}$ g cm^{-3} (Fig. 3a and b) to 0.1 $\times 10^{-3}$ g cm^{-3} (Fig. 3c an d) leads to more pronounced axial profiles (higher conversion per pass) but essentially maintains the shape of the radial profiles, with a less uniform LVRPA profile but still controlled by the chemical reaction kinetics. However, a further increase in the catalyst loading to 0.5 $\times 10^{-3}$ g cm^{-3} (Fig. 3e and f) leads to substantially different radial profiles of the viable bacteria concentration. In this case, the LVRPA (and consequently the reaction rate) near the irradiated wall is so high that leads to a total inactivation of bacteria whereas the opposite wall remains in the dark and no inactivation activity is produced despite the high residence time near the wall.

Fig. 4 schematizes the process, comparing the bacterial concentration, radiation absorption and reaction rate profiles under low and high catalyst loading conditions. As the concentration of bacteria will be always lower near the irradiated wall, mass transport phenomena should play an important role, especially under laminar flow regime, in which bacterial transport takes place by a

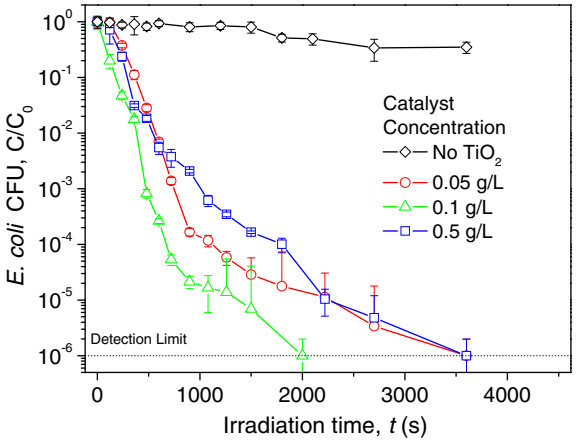

Fig. 5. Experimental results for the photocatalytic inactivation of *E. coli* at the bench scale reactor operating with increasing catalyst concentrations.

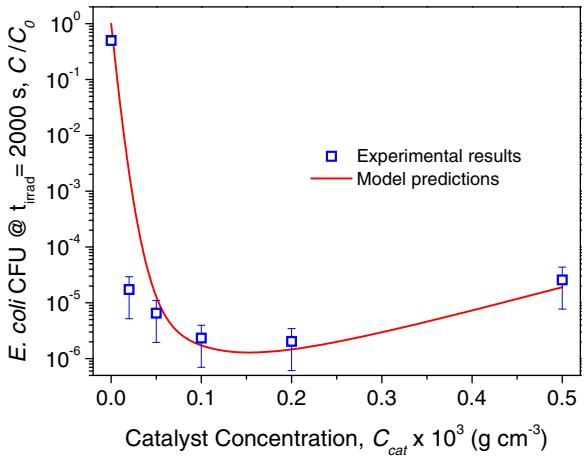

Fig. 6. Comparison between model predictions and interpolated experimental results for the remaining concentration of viable bacteria after 2000 s of irradiation as a function of catalyst concentration.

diffusion mechanism. The relative importance of the mass transport step onto the global kinetics of the process would depend on the catalyst concentration. For low catalyst loadings, the profiles would be not so pronounced, whereas for high catalyst loadings strongly non-uniform profiles will be obtained both for reaction rates and for bacterial concentrations leading to a very likely mass transport control of the process. As mentioned before, this phenomenon could also appear in the photocatalytic oxidation of chemical pollutants, but at much higher TiO_2 concentration values than those predicted in the inactivation of *E. coli*. Actually, concentration profiles have been reported to have a minor effect on the average conversion of chemical pollutants such as cyanide [9]. The reason is that the typical values of the diffusion coefficients of microorganism (e.g. $D^0_{Ecoli-Water} = 9.2 \times 10^{-7} cm^2\ s^{-1}$ [16]) are one order of magnitude lower than those of chemical pollutants (e.g. $D^0_{CN^- -Water} = 1.25 \times 10^{-5}\ cm^2\ s^{-1}$ [19]).

Experimental data obtained in the constructed bench scale reactor (Fig. 5) verified the existence of an optimal catalyst concentration near $0.1 \times 10^{-3}\ g\ cm^{-3}$, with a clear decrease in the photocatalytic inactivation efficiency for $0.5 \times 10^{-3}\ g\ cm^{-3}$ of TiO_2.

Fig. 6 shows that a satisfactory agreement is observed between model predictions and experimental results for the concentration of viable bacteria after a defined irradiation time in the bench scale reactor, specially taking into account the relatively high experimental error of photocatalytic reactions with microorganisms and that the model predictions have been performed without making use of any adjustable parameter. This agreement validates the calculated intrinsic kinetic parameters and the radiation and mass balance models of both the laboratory and the bench scale reactors.

4. Conclusions

The performance of a bench scale photocatalytic reactor, operated under conditions of no perfect mixing, has been simulated to study the disinfection reaction of *E. coli* with titanium dioxide and UV radiation. An absolutely predictive procedure has been employed, based on the intrinsic kinetics and the information about the geometry, irradiation source and operation conditions (catalysts concentration and initial concentration of bacteria). The only experimental information required to be determined at laboratory scale was the intrinsic kinetic parameters of a mechanistic model that takes into account the explicit dependence of the reaction rate on the local volumetric rate of photon absorption. The proposed model has successfully predicted an optimal catalyst concentration in the range $0.1–0.2 \times 10^{-3}\ g\ cm^{-3}$, derived from the significant mass transport control exerted by bacterial diffusion at high TiO_2 loadings. Considering the relatively high experimental error usually found in photocatalytic reactions with microorganisms, a satisfactory agreement was obtained between model predictions and experimental results of viable bacteria concentrations after a defined irradiation time, as a function of catalyst concentration.

Acknowledgements

The authors gratefully acknowledge the financial support of the Ministerio de Ciencia e Innovación of Spain through the Project EMBIOPHOTO (CTM2011-29143-C03-01) and Comunidad de Madrid through the program REMTAVARES (S2009/AMB-1588) and from the Universidad Nacional del Litoral, Agencia Nacional de Promoción Científica y Tecnológica, and Consejo Nacional de Investigaciones Científicas y Técnicas of Argentina. Cristina Pablos also acknowledges Ministerio de Ciencia e Innovación for the FPU grant (AP2008-04567).

References

[1] O.M. Alfano, M.I. Cabrera, A.E. Cassano, Photocatalytic reactions involving hydroxyl radical attack – I. Reaction kinetics formulation with explicit photon absorption effects, J. Catal. 172 (1997) 370–379.
[2] M. Rodríguez, S. Malato, C. Pulgarín, S. Contreras, D. Curcó, J. Giménez, S. Esplugas, Optimizing the solar photo-Fenton process in the treatment of contaminated water. Determination of intrinsic kinetic constants for scale-up, Sol. Energy 79 (2005) 360–368.
[3] I. Salvado-Estivill, D.M. Hargreaves, G. Li Puma, Evaluation of the intrinsic photocatalytic oxidation kinetics of indoor air pollutants, Environ. Sci. Technol. 41 (2007) 2028–2035.
[4] J. Marugán, R. van Grieken, A.E. Cassano, O.M. Alfano, Intrinsic kinetic modeling with explicit radiation absorption effects of the photocatalytic oxidation of cyanide with TiO_2 and silica-supported TiO_2 suspensions, Appl. Catal. B: Environ. 85 (2008) 48–60.
[5] H. de Lasa, B. Serrano, M. Salaices, Photocatalytic Reaction Engineering, Springer, Berlin, 2005.
[6] M.L. Satuf, R.J. Brandi, A.E. Cassano, O.M. Alfano, Scaling-up of slurry reactors for the photocatalytic degradation of 4-chlorophenol, Catal. Today 129 (2007) 110–117.
[7] G. Camera-Roda, F. Santarelli, A rational approach to the design of photocatalytic reactors, Ind. Eng. Chem. Res. 46 (2007) 7637–7644.
[8] G. Li Puma, B. Toepfer, A. Gora, Photocatalytic oxidation of multicomponent systems of herbicides: scale-up of laboratory kinetics rate data to plant scale, Catal. Today 124 (2007) 124–132.
[9] J. Marugán, R. van Grieken, A.E. Cassano, O.M. Alfano, Scaling-up of slurry reactors for the photocatalytic oxidation of cyanide with TiO_2 and silica-supported TiO_2 suspensions, Catal. Today 144 (2009) 87–93.
[10] J. Marugán, R. van Grieken, C. Pablos, M.L. Satuf, A.E. Cassano, O.M. Alfano, Rigorous kinetic modelling with explicit radiation absorption effects of the photocatalytic inactivation of bacteria in water using suspended titanium dioxide, Appl. Catal. B: Environ. 102 (2011) 404–416.
[11] J. Marugán, R. van Grieken, C. Sordo, C. Cruz, Kinetics of the photocatalytic disinfection of *Escherichia coli* suspensions, Appl. Catal. B: Environ. 82 (2008) 27–36 (Corrigendum: Appl. Catal. B: Environ. 88 (2009) 582–583).
[12] M.L. Satuf, R.J. Brandi, A.E. Cassano, O.M. Alfano, Experimental method to evaluate the optical properties of aqueous titanium dioxide suspensions, Ind. Eng. Chem. Res. 44 (2005) 6643–6649.
[13] J. Marugán, R. van Grieken, O.M. Alfano, A.E. Cassano, Optical and physicochemical properties of silica-supported TiO_2 photocatalysts, AIChE J. 52 (2006) 2832–2843.
[14] R. van Grieken, J. Marugán, C. Pablos, L. Furones, A. Lopez, Comparison between the photocatalytic inactivation of Gram-positive *E. faecalis* and Gram-negative *E. coli* faecal contamination indicator microorganisms, Appl. Catal. B: Environ. 100 (2010) 212–220.
[15] A.E. Cassano, C.A. Martin, R.J. Brandi, O.M. Alfano, Photoreactor analysis and design: fundamentals and applications, Ind. Eng. Chem. Res. 34 (1995) 2155–2201.
[16] R.M. Ford, R.W. Harvey, Role of chemotaxis in the transport of bacteria through saturated porous media, Adv. Water Resour. 30 (2007) 1608–1617.
[17] I. Michael, E. Hapeshi, C. Michael, D. Fatta-Kassinos, Solar Fenton and solar TiO_2 catalytic treatment of ofloxacin in secondary treated effluents: evaluation of operational and kinetic parameters, Water Res. 44 (2010) 5450–5462.
[18] J.M. Herrmann, Photocatalysis fundamentals revisited to avoid several misconceptions, Appl. Catal. B: Environ. 99 (2010) 461–468.
[19] X. Sun, Y.C. Guan, K.N. Han, Electrochemical behavior of the dissolution of gold–silver alloys in cyanide solutions, Metall. Mater. Trans. B 27 (1996) 355–361.